LIMNOLOGY
and
OCEANOGRAPHY

ASLO

Limnol. Oceanogr. 62, 2017, 1526–1540
© 2017 The Authors Limnology and Oceanography published by Wiley Periodicals, Inc.
on behalf of Association for the Sciences of Limnology and Oceanography
doi: 10.1002/lno.10515

Light absorption by phytoplankton in the North Pacific Subtropical Gyre

Ricardo M. Letelier,[1,2]* Angelicque E. White,[1,2] Robert R. Bidigare,[2] Benedetto Barone,[2,3] Matthew J. Church,[2,3,4] David M. Karl[2,3]

[1]College of Earth, Ocean, and Atmospheric Sciences, Oregon State University, Corvallis, Oregon
[2]Daniel K. Inouye Center for Microbial Oceanography: Research and Education, Honolulu, Hawaii
[3]Department of Oceanography, University of Hawaii, Honolulu, Hawaii
[4]Flathead Lake Biological Station, University of Montana, Polson, Montana

Abstract

To constrain the energy fueling photosynthesis in the North Pacific Subtropical Gyre (NPSG) we characterize the variability of phytoplankton absorption spectra in conjunction with that of the light field at Station ALOHA (22°45′N, 158°00′W). Furthermore, we decompose the phytoplankton absorption into photosynthetic and photoprotective components based on high-performance liquid chromatography pigment analysis. Between January 2006 and December 2012 the variability in chlorophyll-specific absorption (a^*_ϕ) above the deep chlorophyll maximum (DCM) layer was driven by changes in photoprotective carotenoid concentrations while the chlorophyll-specific absorption of photosynthetic pigments ($a^*_{\phi(\mathrm{PSP})}$) remained nearly constant with a mean (± SD) value of 0.008 ± 0.001 m^2 (mg chl a)$^{-1}$. In contrast, below the DCM layer changes in a^*_ϕ resulted from increases in the relative contribution of photosynthetic pigments with depth, suggesting that the constancy in $a^*_{\phi(\mathrm{PSP})}$ above the DCM layer is controlled by nutrient limitation. While the daily photon fluxes absorbed by photosynthetic pigments in the upper 45 m did not vary at a seasonal scale, averaging 0.45 ± 0.12 mol quanta m^{-2} d^{-1} in winter and 0.46 ± 0.10 mol quanta m^{-2} d^{-1} in summer, when integrated over the upper 200 m these fluxes ranged from 0.64 ± 0.16 to 0.79 ± 0.19 mol quanta m^{-2} d^{-1} in winter and summer, respectively. Based on the rate of photons trapped by the photosynthetic pigments and on the seasonal euphotic zone depth integrated gross O_2 evolution rates derived from $H_2^{18}O$ in situ incubations we estimate a mean photosynthetic yield of ~0.1 mol O_2 evolved per mol quanta absorbed by photosynthetic pigments.

In the open ocean, the capture rate of photons by the light harvesting systems of phytoplankton assemblages sets an upper limit to photoautotrophic productivity. However, the fraction of this harvested radiant flux converted into chemical energy—in the form of a proton gradient and an electric potential across a membrane—is dependent on the pigment composition of these harvesting systems (Raven and Geider 2003). Furthermore, an even smaller fraction of the captured energy is stored in the form of organic matter (i.e., net primary production; Emerson 1958; Morel 1978; Woźniak et al. 2003). For this reason, to constrain estimates of pelagic primary productivity and improve our characterization of the coupling between energy fluxes and the transformation of bio-elements, we need to understand and quantify how environmental factors affect the pigment composition of phytoplankton assemblages and how this pigment composition translates into photosynthetic activity.

Aquatic pelagic photosynthesis takes place in a realm where environmental factors such as temperature or nutrient and light availability affect the trapping and conversion of solar radiation into organic matter (Geider et al. 1997; Marra et al. 2000). In particular, phytoplankton cells are exposed to high variability in the intensity and spectral quality of solar radiation (Cullen and Lewis 1988; Karl et al. 2002; Bidigare et al. 2014). Superimposed on the seasonal and diurnal patterns in solar radiation, phytoplankton can experience rapid changes in the availability of light due to the passage of clouds and vertical displacements in the water column driven by mixing and isopycnal migrations (Karl et al. 2002; Huisman et al. 2006). Although light is abundant in the

*Correspondence: letelier@coas.oregonstate.edu

Additional Supporting Information may be found in the online version of this article.

This is an open access article under the terms of the Creative Commons Attribution License, which permits use, distribution and reproduction in any medium, provided the original work is properly cited.

well-lit upper layer of the open ocean, its intensity decays rapidly with depth due, primarily, to the attenuation of solar radiation by seawater and its particulate components (Smith et al. 1989). In addition, the spectral distribution of light changes with depth as a result of the absorption and scattering properties of water itself, as well as those of particulate and dissolved materials in the water (Kirk 1994). In this variable light environment, phytoplankton taxa have evolved strategies to maximize the capture of photons under light-limiting conditions and to prevent photodamage when the absorbed light energy exceeds the capacity of the photosynthetic apparatus to funnel it toward the production of organic matter (Raven and Geider 2003; Mackey et al. 2008). The timescales for pigment-based acclimations range from seconds-minutes in the case of xanthophyll cycling and state transition shifts, minutes-hours for the synthesis of photoprotective carotenoids, and hours-days for the synthesis of light-harvesting pigments (Ferris and Christian 1991).

In addition to solar irradiance variability, phytoplankton assemblages experience strong temporal and vertical gradients in nutrient availability. This is particularly important in the vast marine oligotrophic regions where the carrying capacity in the upper layers of the water column is chronically nutrient limited (Margalef 1978; Moore et al. 2013). In these oceanic environments the daily-integrated photon flux can vary by two orders of magnitude between the sea surface and the top of the nutricline—the depth at which ambient nutrient concentrations begin to increase; this depth is usually found at or below 90 m depth in the North Pacific Subtropical Gyre (NPSG) and is closely associated with the position of a DCM layer (Letelier et al. 2004). Hence, open ocean oligotrophic regions provide us with the opportunity to study how the photon absorption efficiency of natural phytoplankton assemblages varies along temporal and vertical light gradients under nutrient limiting conditions.

Over the past 28 years—and at nearly monthly intervals—the Hawaii Ocean Time-series (HOT) program has characterized the physics and the biogeochemistry of the water column at Station ALOHA (A Long-term Oligotrophic Habitat Assessment; Karl and Lukas 1996; Church et al. 2013), located at 22°45′N, 158°00′W in the NPSG. In this study we analyze how the spectral absorption of phytoplankton varies with depth and season in this oligotrophic habitat. Based on these observations and concomitant measurements of light distributions throughout the euphotic zone we derive the mean total photon flux absorbed by phytoplankton for winter and summer months to help constrain estimates of the theoretical maximum gross primary production in the NPSG.

Methods

Depth profile of irradiance (*E*)

As part of each HOT cruise, measurements of surface photosynthetically active radiation (PAR) are made using a LI-COR quantum cosine collector (400–700 nm) and data logger (models LI-192SA and LI-1000, respectively). The sensor is positioned above the deck to minimize the influence of shadows from the ship's superstructure. Irradiance is logged throughout the day; readings are averaged in 10 min intervals.

Since May 2009 (HOT cruise # 210), routine deployments of a Satlantic Hyperpro-II have been performed around local noon time to determine the light attenuation and characterize the spectral distribution of irradiance (350–800 nm, 10 nm resolution) in the upper 200 m of the water column. The vertical diffuse attenuation coefficient for PAR (k_d[PAR], m^{-1}) is derived from the ratio of the wavelength integrated downwelling irradiance at depth (E_d[z]) to that of surface downwelling irradiance (E_s) between 400 and 700 nm according to Beer–Lambert–Bouguer law (Eq. 1), following the conversion of the instrument irradiance units from W to quanta s^{-1}.

$$k_d(\mathrm{PAR})_{(0-z)} = \ln\left(\frac{\int_{400}^{700} E_d(z,\lambda)\ d(\lambda)}{\int_{400}^{700} E_s(0,\lambda)\ d(\lambda)}\right)/(-z) \quad (1)$$

where z is depth, $k_d(\mathrm{PAR})_{(0-z)}$ is the mean attenuation coefficient between the surface and depth z, $E_d(z,\lambda)$ is the irradiance at depth z and wavelength λ, and $E_s(0, \lambda)$ is the surface irradiance at wavelength λ. A daily integrated spectrally resolved photon flux at depth is calculated from:

$$\mathrm{PAR}_{0(z)} = 1.2 \times \mathrm{PAR}_{(0+)}\ e^{-\left[k_d(\mathrm{PAR})_{(0-z)} \times z\right]} \quad (2)$$

$$E_{(z,\lambda)\mathrm{day}} = \mathrm{PAR}_{0(z)} \times \frac{E_d(z,\lambda)}{\int_{400}^{700} E_d(z,\lambda)\ d(\lambda)} \quad (3)$$

Where, $\mathrm{PAR}_{(0+)}$ is the daily integrated downwelling PAR measured at the surface and $\mathrm{PAR}_{0(z)}$ is the calculated scalar (downwelling + upwelling) PAR at depth. To convert from downwelling and planar to scalar photon flux we applied a factor of 1.2 (Woźniak et al. 2003). $E_{(z,\lambda)\mathrm{day}}$ is the daily integrated scalar photon flux at depth z and wavelength λ. See Table 1 for a summary list of the nomenclature used.

Prior to May 2009, water column k_d and $\mathrm{PAR}_{0(z)}$ values were characterized with a multispectral Profiling Radiance Reflectance (PRR-600) unit and a PRR-610 surface reference radiometer (Biospherical Instruments; see Letelier et al. 2004). For these cruises (HOT cruises #177 through 209) $E_{(z,\lambda)\mathrm{day}}$ spectra were derived by spectrally weighting the PRR derived $\mathrm{PAR}_{0(z)}$ with the mean spectral distribution of the relative downwelling irradiance at the corresponding standard sampling depths calculated from all Hyperpro-II deployments at Station ALOHA between 2009 and 2014 (Supporting Information Fig. S1).

Phytoplankton spectral absorption

The seasonal and vertical variability in phytoplankton absorption spectra normalized to chlorophyll *a* (chl *a*) concentration (a_Φ^*) has been characterized since January 2006 (HOT cruise # 177). During each cruise 4–10 L water samples

Table 1. List of symbols with their respective units.

Symbol	Units	Description
$a_{\phi(\mathrm{HPLC})}$	m^{-1}	Absorption coefficient of phytoplankton derived from HPLC pigment reconstruction
$a_{\phi(\mathrm{QFT})}$	m^{-1}	Absorption coefficient of phytoplankton derived from quantitative filter technique
a_{CDOM}	m^{-1}	Absorption coefficient of colored dissolved organic matter
a^*_ϕ	m^{-1} (mg chl *a* m^{-3})$^{-1}$	Total chl *a*-specific absorption coefficient
	same as m^2 (mg chl *a*)$^{-1}$	
$a^*_{\phi(\mathrm{PSP})}$	m^2 (mg chl *a*)$^{-1}$	chl *a*-specific absorption coefficient attributed to photosynthetic pigments
$a^*_{\phi(\mathrm{PPC})}$	m^2 (mg chl *a*)$^{-1}$	chl *a*-specific absorption coefficient attributed to photoprotective carotenoids
$\bar{a}^*_\phi$	m^2 (mg chl *a*)$^{-1}$	chl *a*-specific absorption coefficient weighted by the in situ spectral distribution of PAR
$E_{(z)}$	mol quanta m^{-2} s^{-1}	Spectral irradiance at depth *z*
$E_{\mathrm{d}(z)}$	mol quanta m^{-2} s^{-1}	Downward irradiance at depth *z*
E_s	mol quanta m^{-2} s^{-1}	Surface irradiance
k_d	m^{-1}	Diffuse attenuation coefficient for E_d
λ	nm	Wavelength
$\mathrm{PAR}_{(0+)}$	mol quanta m^{-2} day^{-1}	Daily integrated sea surface downwelling photosynthetically available radiation
$\mathrm{PAR}_{0(z)}$	mol quanta m^{-2} day^{-1}	Daily integrated scalar photosynthetically available radiation at depth *z*
Φ	mol (mol quanta)$^{-1}$	Quantum yield of photosynthesis
z	m	Depth

were collected at discrete depths (5, 25, 45, 75, 100, 125, 150, and 175 m) using 12-L polyvinyl chloride sampling bottles attached to a rosette sampler equipped with a conductivity-temperature-pressure (CTD) Sea-Bird SBE911-plus system. Particulate matter in each sample was concentrated onto a 25-mm glass fiber filter (Whatman GF/F) at sea and stored in a tissue culture capsule at either −80°C or in liquid nitrogen for the subsequent characterization of phytoplankton pigments and determination of particulate spectral absorption at our shore-based laboratories.

Particulate spectral absorption was determined using the quantitative filter technique (QFT) described by Kishino et al. (1986). Frozen GF/F filters were placed onto a slide with 200 μL filtered sea water (FSW) and allowed to thaw for ~5–10 min in the dark prior to reading the total particle absorption spectrum (400–800 nm) on a Cary UV-VIS 300 double beam spectrophotometer. To distinguish between the absorption from detritus and that from phytoplankton photosynthetic pigment apparatus, lipid soluble phytoplankton pigments were extracted from the sample by slowly filtering 15 mL of methanol (MeOH) through each filter, subsequently extracting with MeOH for 1 h in the dark, and a final slow filtration with 100 mL MeOH. Each sample was rinsed twice with 5 mL FSW prior to obtaining a reading of the detrital absorption spectrum in the spectrophotometer. Baseline corrections were derived from filter blanks run routinely throughout the day to monitor potential baseline shifts. In addition, for each absorption spectrum determination, the mean reading between 750 and 800 nm was subtracted. Phytoplankton pigment absorption was estimated from the difference between the total and the detrital absorption spectra after correcting for a filter path length amplification (β) factor (Mitchell 1990). To quantify this β factor, several methods were compared, including Mitchell (1990), Bricaud and Stramski (1990) and Roesler (1998). Based on the calculation of the chl-specific absorption at 676 nm derived from normalizing the spectral absorption to the chl *a* concentration value in a subset of our samples we concluded that a value of 2 (as proposed by Roesler 1998) was appropriate for the range of optical density values observed in our filtered samples (data not shown).

Phytoplankton pigments

Samples for pigment analysis were collected, filtered, and preserved in the same manner as those collected for the QFT. Pigment concentrations were estimated based on high-performance liquid chromatography (HPLC) using the method described by Bidigare et al. (2005). Briefly, samples were extracted in 3 mL 100% HPLC grade acetone (Fisher Scientific) at 4°C in the dark for 24 h. As an internal standard, 50 μL of a known canthaxanthin concentration was added to each sample. Following extraction, samples were centrifuged for 5 min at 1500 × *g* to sediment filter and cellular debris. One mL of the final extract was mixed with 0.3 mL HPLC grade water and injected onto a Varian 9012 HPLC system equipped with a Varian 9300 autosampler, a Timberline column heater (26°C) and Spherisorb 5 μm ODS2 analytical (4.6 × 250 mm) column and the corresponding guard cartridge. Pigments were detected with a ThermoSeparation UV2000 detector (λ = 436 and 450 nm). A ternary solvent system was employed for HPLC pigment analysis: eluent A (MeOH : 0.5 M ammonium acetate, 80 : 20), eluent B (acetonitrile:water, 87.5 : 12.5), and eluent C (ethyl acetate). Pigment peaks were identified by comparing their retention times with those of pigment

standards provided by DHI Lab Products (Hørsholm, Denmark) and extracts prepared from phytoplankton reference cultures. Pigment concentrations were calculated using internal and external standards, and expressed as concentrations (mg pigment m^{-3} of filtered seawater).

Phytoplankton spectral absorption reconstruction from pigment composition

For each HPLC sample, the phytoplankton spectral absorption was reconstructed from HPLC pigment analysis following Bidigare et al. (1990). To account for packaging effect we combined the empirical relationship proposed by Woźniak et al. (1999) between chl *a* concentration and phytoplankton cell size with the pigment package effect's spectral function proposed by Morel and Bricaud (1981; also see Le et al. 2008).

Although collected in separate casts, phytoplankton absorption spectra derived from the QFT display a consistent overestimation at 400 nm relative to that from the corresponding HPLC pigment reconstructions. This overestimation has been reported in previous studies by Nelson et al. (1993) and Bricaud et al. (2004), who suggested that it could result from some unknown and missing pigments. However, in our study the magnitude of this overestimation decreased exponentially with increasing wavelength. Based on observations by Karl et al. (1998) and Cetinić et al. (2012) we suggest that a variable residual amount of colored dissolved organic matter (CDOM), or some other detrital component with a similar spectral signature, may have been retained by the filters prior to the MeOH wash. To correct this systematic offset a CDOM contribution to each QFT absorption spectrum was calculated as:

$$a_{\mathrm{CDOM}}(\lambda) = \left[a_{\phi(\mathrm{QFT})}(400) - a_{\phi(\mathrm{HPLC})}(400)\right]^{-0.014(\lambda-400)} \quad (4)$$

where $a_{\mathrm{CDOM}}(\lambda)$ is the absorption by CDOM—or similar detrital matter—at wavelength λ, while $a_{\Phi\ (\mathrm{QFT})}(400)$ and $a_{\Phi\ (\mathrm{HPLC})}(400)$ are the phytoplankton pigment absorption at 400 nm derived from the quantitative filter technique approach and HPLC pigment reconstruction, respectively. The selected CDOM spectral slope coefficient (−0.014) corresponds to the mean value reported by Bricaud et al. (1981) from samples collected in diverse marine environments. CDOM corrected $a_{\Phi\ (\mathrm{QFT})}$ spectra were obtained by removing the a_{CDOM} contribution to the detritus corrected spectrum (Fig. 1).

For each QFT sample, the chl *a* concentration was calculated based on the linear regression of the CDOM corrected spectral absorption line height at 676 nm of all samples versus the monovinyl + divinyl chl *a* concentration from their corresponding HPLC samples (Davis et al. 1997; Boss et al. 2007). From this analysis we obtained a mean $a^*_{\phi(\mathrm{QFT})}(676)$ of 0.0238 (±0.0012) m^{-2} (mg chl $a)^{-1}$ ($r^2 = 0.80$; Supporting Information Fig. S2), a value consistent with observations in oligotrophic waters reported in Figure 1 of Bricaud et al. (1995). The QFT chl-specific absorption at any specific wavelength ($a^*_{\phi(\mathrm{QFT})}(\lambda)$) was obtained from the QFT spectral distribution of phytoplankton pigment absorption divided by the chl *a* concentration derived from QFT absorption line height, as described above. Overall, the spectral average of QFT chl-specific absorption ($a^*_{\phi(\mathrm{QFT})}$) for the 400–750 nm range was strongly correlated to that derived from HPLC pigment reconstruction ($a^*_{\phi(\mathrm{HPLC})}$) with a slope not significantly different than unity (Fig. 2).

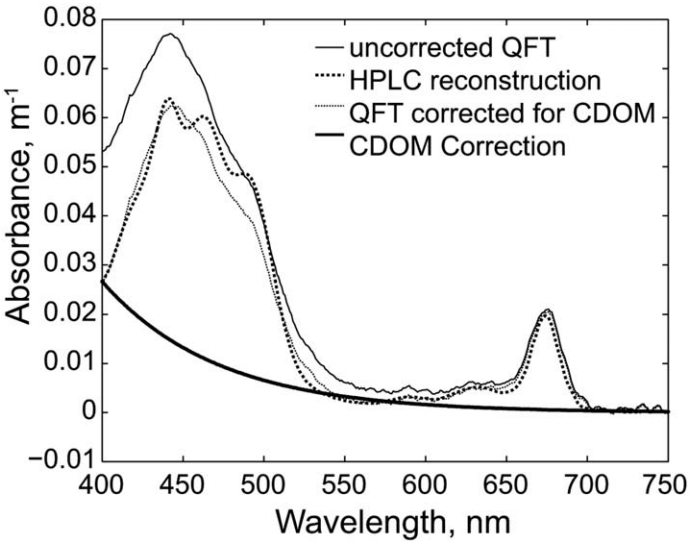


Fig. 1. Comparison between absorption spectrum derived from HPLC pigment reconstruction and corrected for packaging effect (——), QFT pigment fraction uncorrected for residual CDOM (·····), CDOM correction (——), and CDOM corrected pigment QFT absorption (– – – –).

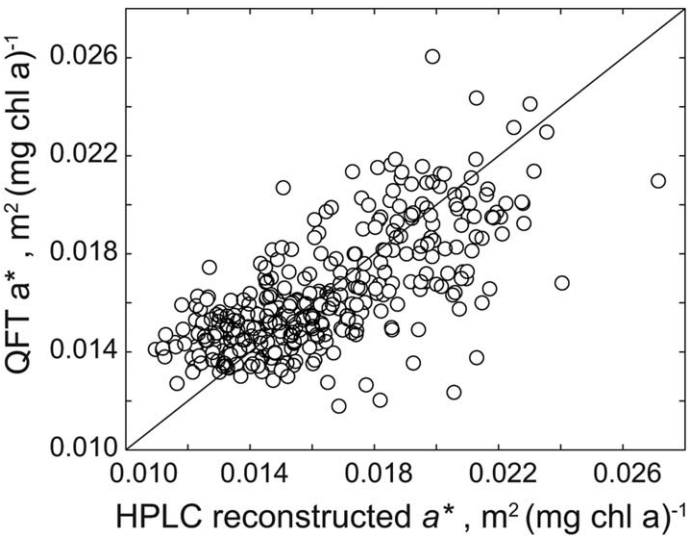


Fig. 2. Relationship between CDOM corrected chl-specific absorption (400–750 nm) derived from QFT and chl-specific absorption from HPLC pigment reconstruction and corrected for packaging effect.

Finally, the depth of the DCM layer was estimated based on the maximum chl fluorescence observed at depth from the continuous trace recorded by a Sea-Point fluorometer connected to the Sea-Bird CTD package mounted on the sampling rosette. This DCM layer was used to distinguish between a nutrient limited region (above the DCM layer) and a nutrient sufficient (below the DCM layer) according to Letelier et al. (2004).

Results

Over the course of this study (January 2006 through December 2012), daily-integrated surface PAR recorded during HOT cruises varied by threefold, with a maximum value of 48.4 mol quanta m^{-2} d^{-1} measured on 30 May 2012 (HOT cruise # 242) and a minimum of 15.2 mol quanta m^{-2} d^{-1} registered on 3 December 2012 (HOT cruise # 248). Surface PAR displayed a significant seasonal cycle with highest average monthly values (>42 mol quanta m^{-2} d^{-1}) observed from June through August and the lowest values (<29 mol quanta m^{-2} d^{-1}) recorded in November through January. Based on the observed seasonal PAR cycle we define June through August as summer months and November through January as winter months.

The CDOM corrected $a^*_{\phi(\mathrm{QFT})}$ spectra at Station ALOHA display two characteristic distributions as a function of depth. Samples collected above the DCM (< 90 m) were characterized by a maximum at ~ 440 nm and a shoulder at 490 nm. In contrast, below the DCM (> 110 m), $a^*_{\phi(\mathrm{QFT})}$ displays a pronounced absorption peak at ~ 485 nm, reflecting a significant increase in the concentration of photosynthetic pigments relative to that of chl *a* (Fig. 3). Furthermore, the chl *a* concentration and its specific absorption, as derived from the QFT method, display opposite seasonal cycles in the upper 45 m: while the chl *a* concentration decreases during the summer months (Fig. 4A), $a^*_{\phi(\mathrm{QFT})}$ peak during summer (June–August) relative to winter (November–January) (Fig. 4B). This seasonal pattern appears to reverse at and below the DCM layer.

The vertical and seasonal patterns in $a^*_{\phi(\mathrm{QFT})}$ reflect the relative distribution of the dominant phytoplankton pigments derived from HPLC (Fig. 5): In the upper water column the observed decrease in $a^*_{\phi(\mathrm{QFT})}$ with increasing depth can be attributed to the vertical distribution patterns of zeaxanthin (zea) relative to chl *a* (Fig. 5C). In addition, the seasonal pattern of $a^*_{\phi(\mathrm{QFT})}$ in this upper layer can only be explained by changes in the relative contribution of photoprotective pigments since the relative contribution by photosynthetic pigments remains constant (Fig. 6). In contrast, the increase in $a^*_{\phi(\mathrm{QFT})}$ below 100 m depth correlates with increases in chl *b*, 19′-hexanoyloxyfucoxanthin (19′-hex) and 19′-butanoyloxyfucoxanthin (19′-but)(Fig. 5B).

The contribution of photosynthetic and photoprotective pigments to the phytoplankton spectral absorption ($a^*_{\Phi(\mathrm{PSP})}$ and $a^*_{\Phi(\mathrm{PPC})}$, respectively) can be derived from pigment concentrations (Fig. 5) and the in vivo spectral absorption of each pigment (Bidigare et al. 1990; Babin et al. 1996; Allali et al. 1997). Based on this approach we estimate that in the upper 45 m of the euphotic zone photosynthetic pigments (monovinyl and divinyl chls *a* and *b*, chl *c*, fucoxanthin (fuco), peridinin, 19′-hex, and 19′-but; Fig. 5A,B) contribute 36% ± 5% of the total a^*_{Φ} during summer months and 50% (±7%) in winter; in contrast, this contribution increases to ~80% ± 4% below the DCM layer and remains constant across seasons (Fig. 6B). The remaining absorption is attributed to photoprotective carotenoids, comprised primarily by zea, with lesser contributions by diadioxanthin and $\alpha + \beta$-carotenes (Fig. 5C).

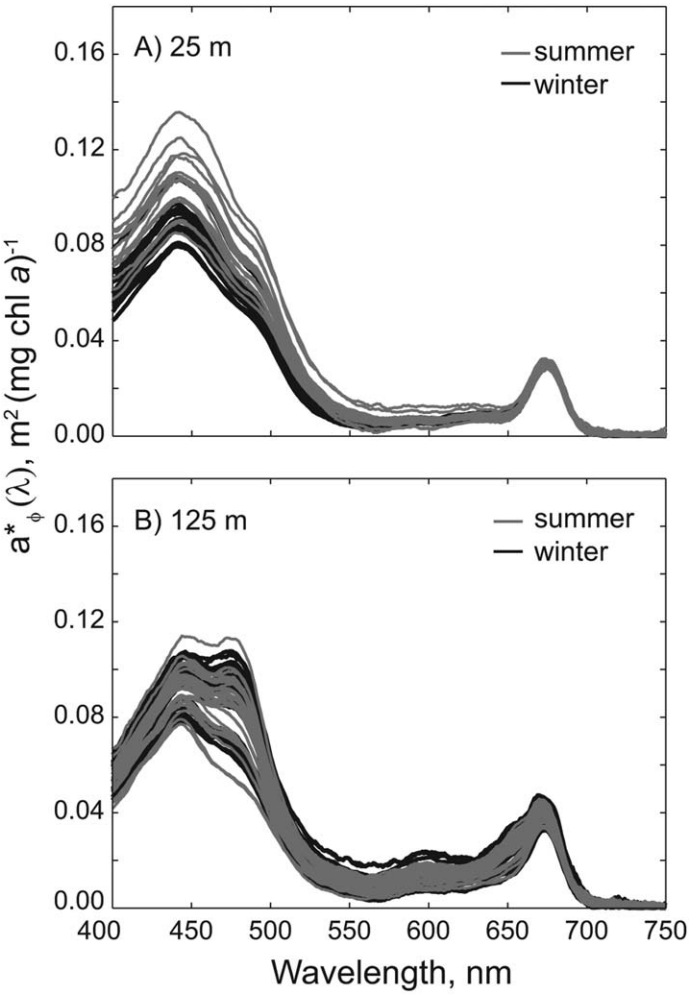


Fig. 3. Ensemble of all summer (grey) and winter (black) QFT derived chl-specific absorption spectra collected at 25 m (upper panel) and 125 m (lower panel).

However, to calculate the photon flux that is actually absorbed by phytoplankton, specific absorption spectra need to be weighted by the in situ spectral composition of the light (Kishino et al. 1986; Sakshaug et al. 1997), which changes with depth (Supporting Information Fig. S1):

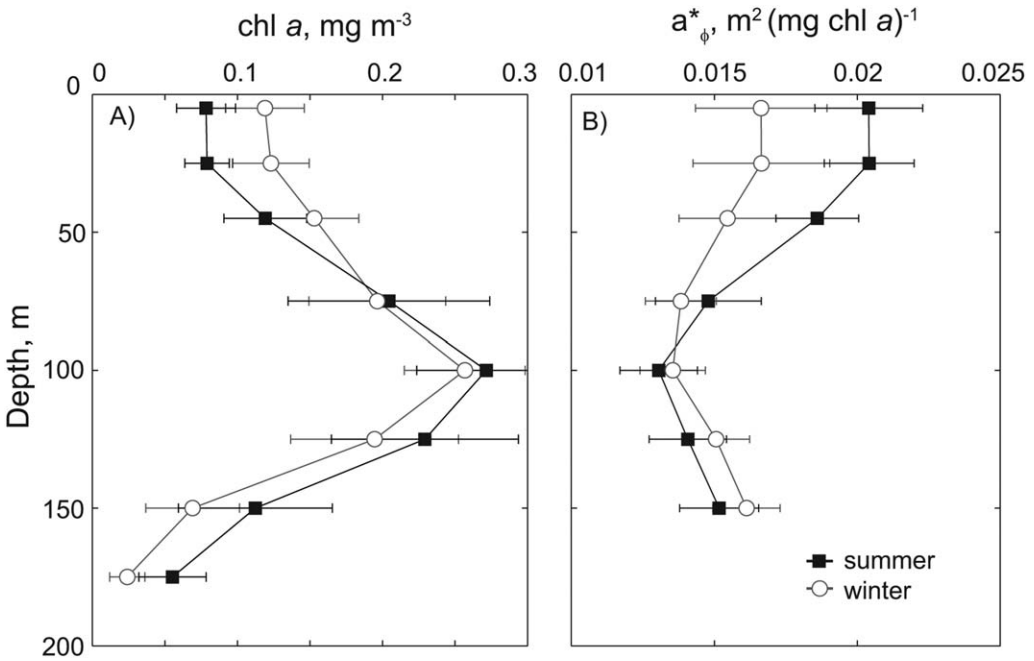


Fig. 4. Depth distribution (mean ± SD) of chl *a* concentrations and chl-specific absorption derived from QFT (open circles = winter and closed squares= summer months).

$$\bar{a}^*_\phi = \frac{1}{\int_{400}^{750} E(\lambda)\ d\lambda} \int_{400}^{750} a^*_\phi(\lambda) \times E(\lambda)\ d\lambda \quad (5)$$

where $\bar{a}^*_\phi$ corresponds to a^*_ϕ weighted by the *in situ* spectral distribution of PAR.

As observed by previous authors (e.g., Kishino et al. 1986; Markager and Warwick 2001), $\bar{a}^*_\phi$ is significantly higher than a^*_ϕ due to the spectral shift of PAR_0 toward the blue region of the spectrum with depth, increasing by a factor of 1.5 at 5 m depth and by a factor of ~ 2.2 at 25 m and below (Fig. 7). For this reason, when compared to a^*_ϕ, the relative contribution of photosynthetic pigments to $\bar{a}^*_\phi$ in surface layers decreases to ~ 30% and 45% for summer and winter, respectively, while remaining close to 80% at depth.

Discussion

The energy trapped by phytoplankton assemblages provides an upper boundary estimate of gross photoautotrophic productivity in a pelagic environment. This flow is linearly dependent on the photosynthetically available radiation (PAR_0) at depth z and time *t*, the corresponding chl *a* concentration [chl *a*] and the chl-specific absorption attributed to photosynthetic pigments ($\bar{a}^*_{\phi(PSP)}$), which provides an estimate of the size of the photosynthetic antenna per reaction center (Dubinsky 1992), as long as the number of chl *a* molecules per photosystem II (PSII) reaction center remains constant (Oxborough et al. 2012). To convert this captured energy into oxygen produced or carbon assimilated we must apply a quantum yield (Φ), which defines the number of oxygen molecules evolved or carbon atoms assimilated into organic matter per photon absorbed:

$$GPP_{(z,t)} = PAR_{0(z,t)} \times [\text{chl } a]_{(z,t)} \times \left(\bar{a}^*_{\phi(PSP)}\right)_{(z,t)} \times \Phi_{(z,t)} \quad (6)$$

While the variability in $PAR_{0(z,t)}$ and $[\text{chl } a]_{(z,t)}$ have been well characterized at Station ALOHA (Letelier et al. 1993, 2004), to date we have a limited understanding of how ($\bar{a}^*_{\phi(PSP)}$) and Φ for oxygen and carbon fluctuate in time and with depth.

Chl-specific absorption variability

In the present study, the phytoplankton spectral absorption derived from both QFT and HPLC pigment reconstruction suggests a consistent decrease in total a^*_Φ with decreasing light levels (increasing depth) in the upper region of the euphotic zone (Fig. 4B and Supporting Information S3). In addition, the decomposition of total a^*_Φ into the absorption contributed by photoprotective carotenoids ($a^*_{\Phi(PPC)}$) and that contributed by photosynthetic pigments ($a^*_{\Phi(PSP)}$) reveals that above the DCM layer the variability in a^*_Φ is driven almost exclusively by changes in the contributions of photoprotective pigments relative to chl *a*. In contrast, it is the change in the relative contribution of photosynthetic pigments that accounts for the increase in total a^*_Φ below the DCM layer (Fig. 8). These results are consistent with previous studies by Sosik and Mitchell (1995) and Allali et al. (1997) who found that the observed

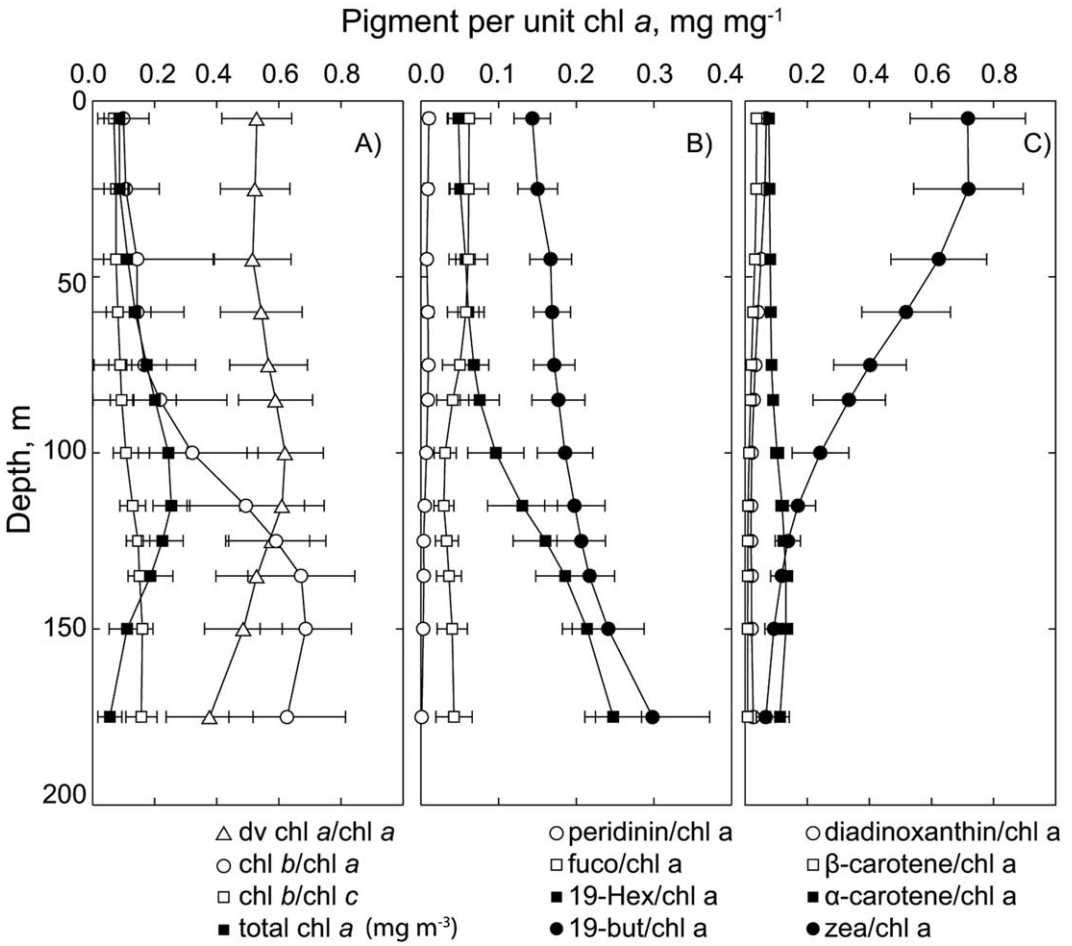


Fig. 5. Depth distribution (mean ± SD) of HPLC derived chl *a* concentrations (mv + dv chl *a*) and that of accessory pigments concentrations relative to that of chl *a*. (**A**) chl pigments (open triangles: [dv chl *a*/total chl *a*], open circles: [chl *b*/total chl *a*], open squares: [chl *c*/total chl *a*], close squares: [total chl *a*]). (**B**) Photosynthetic carotenoids (open circles: [peridinin/total chl *a*], open squares: [fuco/total chl *a*], close squares: [19-hex/total chl *a*], close circles: [19-but/total chl *a*]). (**C**) Photoprotective carotenoids (open circles: [diadinoxanthin/total chl *a*], open squares: [β-carotene/total chl *a*], close squares: [α-carotene/total chl *a*], close circles: zea/total chl *a*]).

variability of a^*_Φ in the upper layers of the water column is dominated by changes in $a^*_{\Phi(\mathrm{PPC})}$.

Several factors contribute to the variability in pigment composition of natural assemblages. These include changes in phytoplankton taxonomic diversity (Margalef 1978; Letelier et al. 1993; Reigman and Rowe 1994), photoacclimation (Deming-Adams 1990; Demers et al. 1991; Falkowski and LaRoche 1991), nutrient limitation (Ketchum et al. 1958; Yentsch and Vaccaro 1958; Watson and Osborne 1979; Latasa 1995), and the role of grazers and viruses in controlling the diversity and abundance of phytoplankton taxa (Latasa et al. 1997; Suttle 2000). At present it may be difficult to quantify the role that each one of these processes plays in the observed temporal and spatial variability in pigment composition at Station ALOHA. Nonetheless, we can try to interpret the observed variability in pigment composition in terms of the response of the full photoautotrophic assemblage to changes in light intensity and nutrient availability.

The chl-specific absorption attributed to photoprotective carotenoids ($a^*_{\Phi(\mathrm{PPC})}$) accounts for approximately 70% of the total absorbed photon flux in the upper layers of the euphotic zone during summer months, decreasing to 55% in winter and to less than 20% below the DCM layer. Increases in the relative concentration of photoprotective carotenoids have been interpreted primarily as an acclimation mechanism aimed at minimizing damage of the photosynthetic apparatus that can arise from exposure to excess light (Deming-Adams 1990; Demers et al. 1991). In addition, some carotenoids play an important role in the mitigation of oxidative stress experienced by cells exposed to light conditions that exceed the processing capability of the photosynthetic apparatus (Cirulis et al. 2013 and references therein). These metabolic responses are consistent with the high concentration of zea observed in surface waters and with increased contributions of photoprotective carotenoids to total a^*_Φ in the upper 45 m depth in summer.

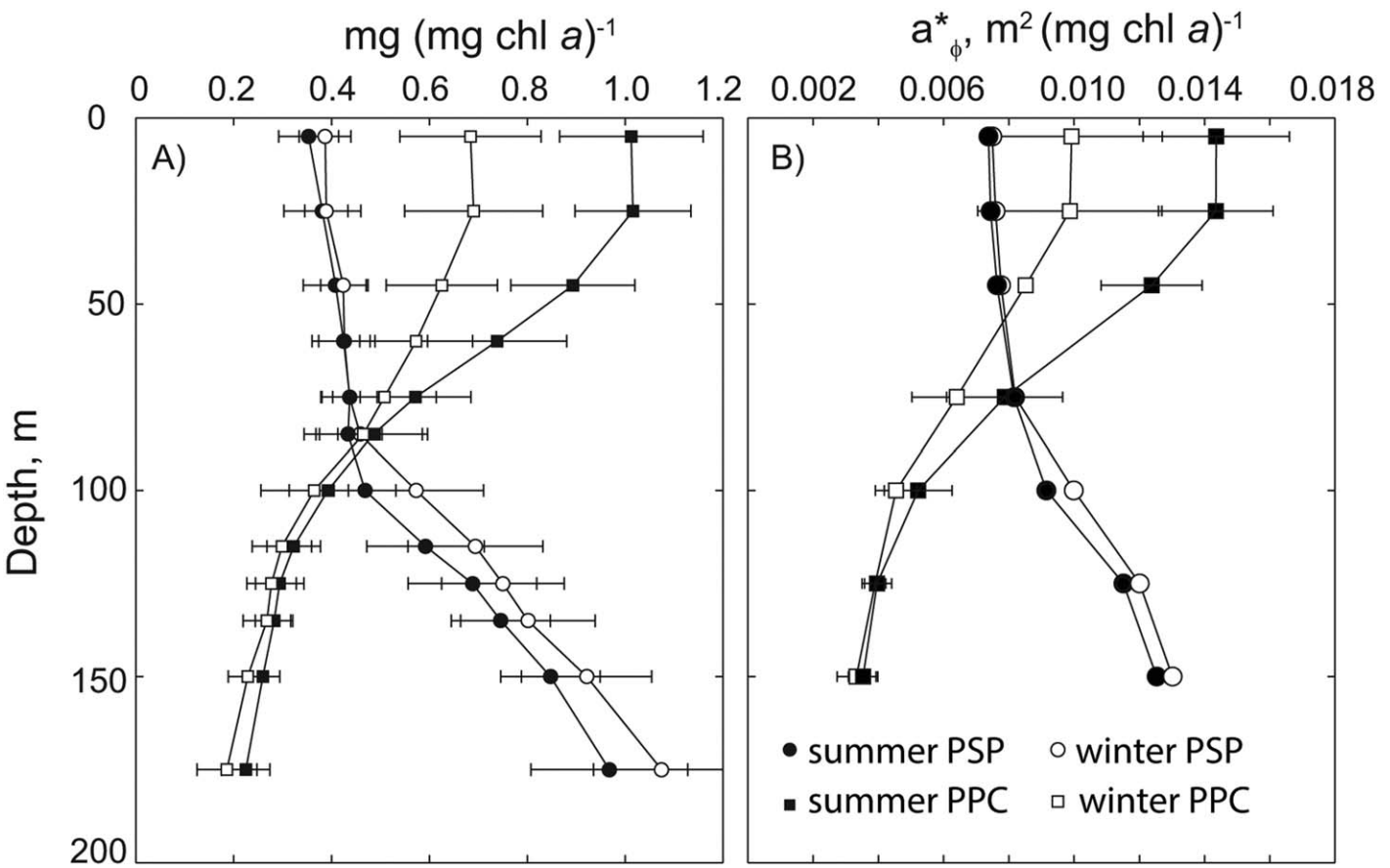


Fig. 6. Relative photosynthetic (circles) and photoprotective (squares) pigments concentration (left panel) and chl-specific absorption (right panel) as a function of depth and season. (Open symbols = winter, close symbols = summer).

The increase in the ratio of photoprotective carotenoids to chl *a* from the DCM layer to below the light saturating region of primary productivity (~45 m, see Letelier et al. 1996) may represent a physiological indicator of nutrient limitation. Several studies (Latasa and Berdalet 1994; Schlüter et al. 1997; Staehr et al. 2002; Přibyl et al. 2016) have documented an increase in carotenoids per unit chl in response to nutrient limitation, even under low light and balanced growth conditions. For example, in a study of variations in cell composition of the haptophyte *Pavlova lutheri* (Droop) grown in chemostats and exposed to high and low light levels, Madariaga and Joint (1992) observed that cells grown under low light and nitrogen (N) or phosphorus (P) limitation triggered a >2.5-fold decrease in chl pigments; in contrast, N limitation increased diadinoxanthin and β-carotene by factors of 3 and 8, respectively. The reason for this relative increase has been attributed to a differential nutrient requirement in the metabolic pathways of chlorophyll pigments versus carotenoids. The common nutrient requirements of different chls may also explain the constancy in $a^*_{\Phi(\mathrm{PSP})}$ above the DCM layer since most of the photosynthetic absorption in this region of the water-column is due to chl pigments with minor contributions from photosynthetic carotenoids (Fig. 5).

The consistency of $a^*_{\Phi(\mathrm{PSP})}$ with depth and season above the DCM layer is somewhat surprising because it suggests that, under nutrient limiting conditions—as those encountered above the DCM layer at Station ALOHA (Letelier et al. 2004), the efficiency of the photosynthetic antennae in absorbing incident photons to fuel algal photosynthesis remains relatively constant over a broad range of PAR intensities. Instead, photoacclimation and photoadaptation in this oligotrophic layer is driven primarily by changes in the concentration of photoprotective carotenoids (Fig. 6) and by changes in the size of the photosynthetic antenna and/or the number of photosynthetic units (PSUs) per volume, as suggested by the change of chl concentration with depth and season (Fig. 5A) and per cell, as evidenced by the observed increase in chl fluorescence per cell in *Prochlorococcus* spp. as PAR decreases (Winn et al. 1995). In these nutrient limited layers the variability in $a^*_{\Phi(\mathrm{PSP})}$ appears to be small compared to that of other photoacclimation and photoadaptation mechanisms. In contrast, increases in $a^*_{\Phi(\mathrm{PSP})}$ with decreasing PAR_0 below the DCM layer seem to confirm

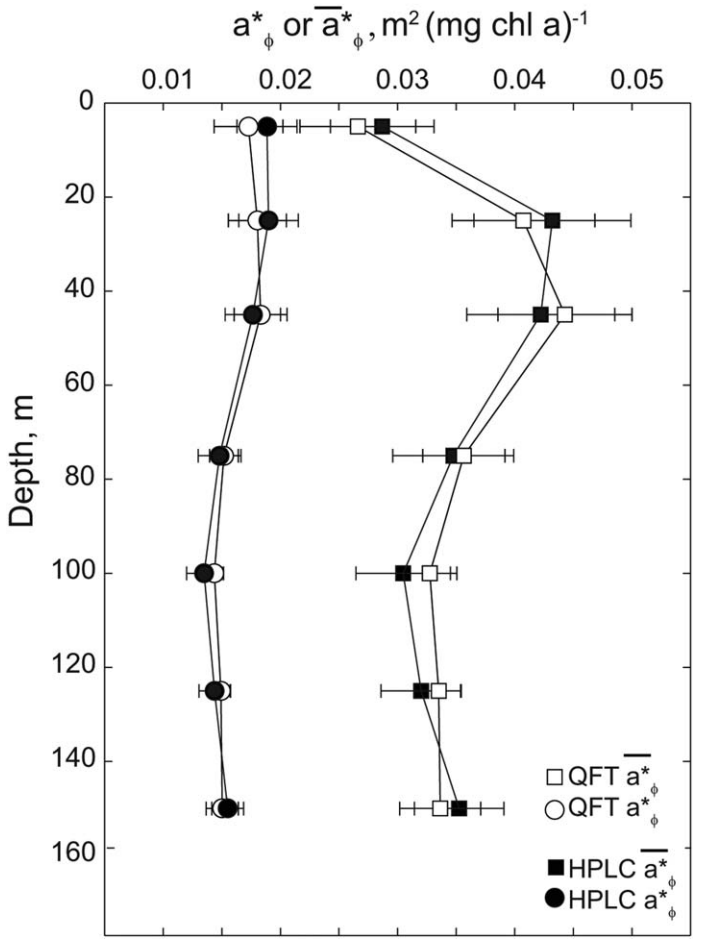


Fig. 7. Depth distribution of total chl-specific absorption unweighted (circles) as well as weighted for the spectral distribution of light (squares). QFT = open symbols, HPLC reconstruction = close symbols.

that changes in the photosynthetic trapping efficiency of incident photons by PSUs are an important driver of photoadaptation in these well stratified layers under light limiting and nutrient replete conditions (Fig. 6).

Seasonal water column phytoplankton light absorption budget

Although Station ALOHA experiences a significant seasonal solar irradiance cycle, with mean daily-integrated surface PAR values in summer months that are 1.5 times greater than those observed in winter, this seasonality does not appear to translate into a summer increase in the photon flux being absorbed by the phytoplankton's photosynthetic pigments in the upper layers of the euphotic zone. When calculating the photon flux absorbed by phytoplankton photosynthetic pigments—as $E(z) \times$ chl a concentration $\times \bar{a}^*_{\phi\,(\mathrm{PSP})}$—we find that winter month 0–45 m mean (± SD) integrated values are approximately 0.45 ± 0.12 mol quanta m^{-2} d^{-1} while in summer the absorbed photon flux averages 0.46 ± 0.10 mol quanta m^{-2} d^{-1} (Table 2, Fig. 9). This apparent lack of an annual cycle in the photosynthetic absorbed energy can be attributed to an inverse seasonal cycle between chl a concentration and daily-integrated solar irradiance, while $\bar{a}^*_{\phi\,(\mathrm{PSP})}$ remains invariant in these upper layers. However, at and below 100 m depth the summer values of light absorption are consistently greater than those measured in winter leading to an euphotic zone integrated (0–200 m) photon flux of 0.79 ± 0.19 mol quanta m^{-2} d^{-1} and 0.64 ± 0.16 mol quanta m^{-2} d^{-1}, respectively.

A comparison of the absorbed photon flux by photosynthetic pigments with the gross oxygen production (GOP) derived from in situ ^{18}O-H_2O incubations can provide a rough estimate of the fraction of absorbed energy being channeled through PSII. Based on near monthly in situ ^{18}O-H_2O incubations carried over a 2-year period (March 2006 through February 2008) Quay et al. (2010) estimated that the mean (± SD) 0–100 m integrated GOP varies between 89 ± 18 and 67 ± 13 mmol O_2 m^{-2} d^{-1} in summer and winter, respectively. These values correspond to approximately $1/10^{\mathrm{th}}$ of absorbed quanta over the same integrated depth range and season (712 and 613 mmol quanta m^{-2} d^{-1}, respectively; Table 2). Although our observations appear to be in good agreement with the canonical photosynthetic quantum efficiency of 0.1 mol O_2 evolved per mol quanta first observed by Emerson (1958), they represent the seasonal ratio between two bulk estimates and may mask the natural variability in the oxygen quantum yield.

Finally, although ($\bar{a}^*_{\phi\,(\mathrm{PSP})}$) remained constant in the upper water column over the extent of this study (2006 through 2012), Karl et al. (2001) suggested that a strong shift toward a prokaryote-dominated phytoplankton community took place between 1975 and 1985 in the region surrounding Station ALOHA. More recently, Corno et al. (2007) and Bidigare et al. (2009) reported the occurrence of a relatively abrupt increase in photosynthetic (chl b, fuco and 19′-hex) and photoprotective (zea) pigment abundance at Station ALOHA during the mid to late 1990s, coincident with a shift in El Nino Southern Oscillation and Pacific Decadal Oscillation climate indices. Hence, we cannot discard the possibility that significant shifts in environmental conditions affect long-term changes in the phytoplankton community structure and the mean photosynthetic functional absorption cross section in this oligotrophic region.

Uncertainties in the photosynthesis photon budget analysis

Our derivation of the photon flux absorbed by phytoplankton assemblages is based on the assumption that the absorption between 400 and 750 nm by photosynthetic pigments derived from HPLC analysis accurately reflects the flow of energy into the photosynthetic reaction centers. However, this photon flux may be underestimated due to several factors. For example, our calculations do not take into account the contribution to the total photon budget of

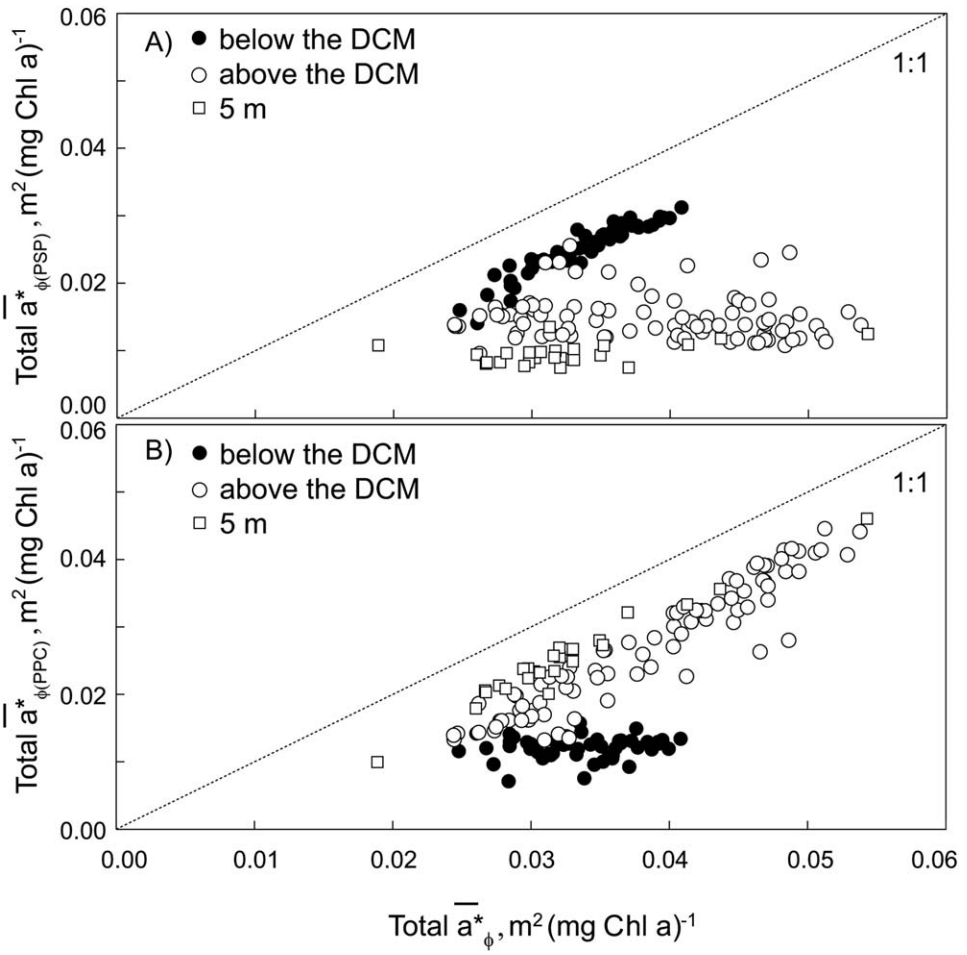


Fig. 8. Chl-specific photosynthetic (upper panel) and photoprotective (lower panel) absorption as a function of total chl-specific absorption. Close symbols = samples collected below the DCM layer; open symbols = sample collected above the DCM layer; open squares = samples collected at 5 m depth.

UV radiation (280–400 nm) and its effect on photosynthesis. Nevertheless, prior studies on natural phytoplankton assemblages suggest that the effect of UV radiation on photosynthetic rates in low latitude oligotrophic regions is negligible (Helbling et al. 1992; Montecino and Pizarro 1995).

Not accounting for the presence of water-soluble photosynthetic pigments in our samples is another potential cause of underestimating the total photon flux absorbed by the phytoplankton assemblage. A close comparison between the CDOM corrected QFT absorption spectra wavelength ($a^*_{\phi(\mathrm{QFT})}$) and that derived from HPLC pigment reconstruction wavelength ($a^*_{\phi(\mathrm{HPLC})}$), identifies a minor deviation centered around 525 nm in some of our samples (Fig. 1), consistent with the presence of phycoerythrin (Bidigare et al. 1989). However, when weighted by the in situ spectral composition of the light (Eq. 5), the photon flux absorption attributed to phycoerythrin for any given sample is less than 1% of the total $\bar{a}^*_{\phi\,(\mathrm{PSP})}$ (data not shown).

A third source of uncertainty we need to consider is the possibility that a small fraction of the energy absorbed by photoprotective pigments is funneled into photosynthesis. In this context, our results suggest that zea accounts for over 90% of the photoprotective carotenoid's absorbance in the upper 45 m (Fig. 5). Based on previous measurements of cellular zea concentrations in *Synechococcus* spp. and *Prochlorococcus* spp. (Bidigare et al. 1989; Moore et al. 1995) and the abundance of these cyanobacteria at Station ALOHA (Campbell and Vaulot 1993; Malmstrom et al. 2010), we conclude that all zea can be ascribed to these taxa in these upper water column layers. The lack of evidence for the transfer of energy from zea to the photosystem in *Synechococcus* spp. and *Prochlorococcus* spp. (Bidigare et al. 1989; Moore et al. 1995) suggests that photoprotective carotenoids do not contribute significantly to the flow of energy into photosynthesis in our study region.

Finally, our sampling approach may miss the contribution of large but rare aggregates, such as *Trichodesmium* spp. colonies that are commonly found in concentrations lower than 0.1 colonies L^{-1} (Letelier and Karl 1996). Furthermore, our analysis does not take into account the energy contribution

Table 2. Winter (November–January) and summer (June–August) mean and (SD) of photosynthetically available radiation (PAR_0), spectrally weighted chlorophyll *a* specific absorption attributed to photosynthetic pigments ($\bar{a}^*_{\phi(PSP)}$), HPLC derived chlorophyll *a* concentration (chl *a*), and absorbed photon flux by photosynthetic pigments at standard sampling depth of the HOT program.

	PAR_0 (mol quanta m^{-2} d^{-1})		$\bar{a}^*_{\phi(PSP)}$ (m^2 (mg chl *a*)$^{-1}$)		[chl *a*] (mg m^{-3})		$PAR_0 \times \bar{a}^*_{\phi(PSP)} \times$ [chl *a*] (Absorbed photon flux) (mmol quanta m^{-3} d^{-1})	
Depth (m)	**Winter**	**Summer**	**Winter**	**Summer**	**Winter**	**Summer**	**Winter**	**Summer**
5	12.5 (2.5)	21.9 (2.4)	0.0097 (0.0009)	0.0093 (0.0008)	0.117 (0.042)	0.067 (0.015)	14.2 (3.1)	13.7 (3.2)
25	5.2 (1.0)	9.4 (1.0)	0.0139 (0.0011)	0.0134 (0.0011)	0.120 (0.043)	0.071 (0.014)	8.7 (2.3)	8.9 (1.7)
45	2.3 (0.4)	4.6 (0.5)	0.015 (0.0016)	0.0137 (0.0015)	0.147 (0.042)	0.099 (0.028)	5.1 (1.4)	6.2 (1.7)
75	0.88 (0.17)	1.87 (0.21)	0.016 (0.0021)	0.015 (0.0012)	0.198 (0.062)	0.177 (0.056)	2.8 (0.7)	5.0 (1.0)
100	0.32 (0.06)	0.71 (0.08)	0.0202 (0.0041)	0.017 (0.0031)	0.253 (0.057)	0.256 (0.049)	1.6 (0.4)	3.1 (0.7)
125	0.096 (0.019)	0.227 (0.026)	0.0253 (0.0030)	0.0229 (0.0040)	0.178 (0.055)	0.24 (0.064)	0.43 (0.09)	1.25 (0.38)
150	0.027 (0.006)	0.068 (0.008)	0.0281 (0.0022)	0.0257 (0.0038)	0.064 (0.036)	0.117 (0.055)	0.049 (0.012)	0.204 (0.071)
Depth Integration							**(mol quanta m^{-2} d^{-1})**	
0–45 m							0.45 (0.12)	0.46 (0.10)
100–200 m							0.033 (0.004)	0.079 (0.012)
0–200 m							0.64 (0.16)	0.79 (0.19)

Depth integration assumes constant absorbed flux in the upper 5 meters and no absorption at 200 m depth.

Fig. 9. Seasonal depth distribution of daily PAR_0 (circles) and photon flux absorbed by photosynthetic pigments (squares). Close symbols = summer; open symbols = winter.

of light driven proton pumps found in some marine heterotrophs. Over the past two decades several studies have suggested that this process may be ubiquitous in the open ocean and can contribute to the metabolic activity of proteorhodopsin-containing bacteria, such as SAR11 (Pelagibacter), SAR86, and SAR116 (Béjà et al. 2001; DeLong and Béjà 2010) which are some of the more abundant taxa in pelagic marine environments. Because these processes are not associated with the evolution of O_2 or NADPH, they will not affect the quantum yield of oxygen evolution or organic matter production. Nevertheless, they may contribute significantly to the total energy budget of the pelagic oligotrophic microbial assemblage.

In spite of these uncertainties, our observations are consistent with results from prior studies. In a synthesis effort to

model phytoplankton spectral absorption distribution as a function of pigment composition Woźniak et al. (2000) concluded that $\bar{a}^*_{\phi\,(\mathrm{PSP})}$: $\bar{a}^*_{\phi}$ varied between 0.3 and ~0.9 in surface layers of oligotrophic and eutrophic regions, respectively. More recently, Lin et al. (2016) combined in situ variable fluorescence and satellite retrieved solar induced fluorescence to conclude that approximately 35% of photons absorbed by phytoplankton in the open ocean are funneled into the photochemistry. Our results suggest that the relative contribution of photosynthetic pigments to $\bar{a}^*_{\phi}$ in the surface layers at Station ALOHA ranges from ~ 30% in summer to ~ 45% in winter.

Conclusions

Our long-term observations at Station ALOHA suggest that, under nutrient limited conditions, such as those that characterize the NPSG, the chl-specific photosynthetic absorption ($\bar{a}^*_{\phi\,(\mathrm{PSP})}$) remains nearly constant over a broad range of light conditions. This constancy, which reflects an apparent lack of plasticity of the functional cross section of PSII (σ_{O2}), allows a straightforward approach to estimate the gross oxygen evolution in the upper layers of subtropical oligotrophic oceanic regions based on daily sea surface solar irradiance and chl *a* concentration. However, although this approach may provide an upper theoretical estimate of gross photoautotrophic production, the challenge remains in understanding what controls the variability in the fraction of photosynthetic energy that is channeled into the gross synthesis and, ultimately, into the net storage of organic matter in this marine oligotrophic environment.

References

Allali, K., A. Bricaud, and H. Claustre. 1997. Spatial variations in the chlorophyll-specific absorption coefficients of phytoplankton and photosynthetically active pigments in the Equatorial Pacific. J. Geophys. Res. **102**: 12413–12423. doi:10.1029/97JC00380

Babin, M. A., Morel, H. Claustre, A. Bricaud, Z. Kolber, and P. G. Falkowski. 1996. Nitrogen- and irradiance-dependent variations of the maximum quantum yield of carbon fixation in eutrophic, mesotrophic and oligotrophic marine systems. Deep-Sea Res. I **43**: 1241–1272. doi:10.1016/0967-0637(96)00058-1

Béjà, O., E. N. Spudich, J. L. Spudich, M. Leclerc, and E. F. DeLong. 2001. Proteorhodopsin phototrophy in the ocean. Nature **411**: 786–789. doi:10.1038/35081051 [11459054]

Bidigare, R. R., O. Schofield, and B. B. Prézlin. 1989. Influence of zeaxanthin on quantum yield of photosynthesis of *Synechococcus* clone WH7803 (DC2). Mar. Ecol. Prog. Ser. **56**: 177–188. doi:10.3354/meps056177

Bidigare, R. R., M. E. Ondrusek, J. H. Morow, and D. A. Kiefer. 1990. In vivo absorption properties of algal pigments, p. 90–102. *In* R. W. Spinrad [ed.], Ocean Optics X, Proc. Soc. Photo-opt. Instrum. Eng., V. **1302**.

Bidigare, R. R., L. Van Heukelem, and C. C. Trees. 2005. Analysis of algal pigments by high-performance liquid chromatography, p. 327–345. *In* R. A. Andersen [ed.], Algal culturing techniques. Academic Press.

Bidigare, R. R., and others. 2009. Subtropical ocean ecosystem changes forced by North Pacific climate variations. J. Plankton Res. **31**: 1131–1139. doi:10.1093/plankt/fbp064

Bidigare, R. R., F. R. Buttler, S. J. Christensen, B. Barone, D. M. Karl, and S. T. Wilson. 2014. Evaluation of the utility of xanthophyll cycle pigment dynamics for assessing upper ocean mixing processes at Station ALOHA. J. Plankton Res. **36**: 1423–1433. doi:10.1093/plankt/fbu069

Boss, E. S., C. Collier, G. Larson, K. Fennel, and W. S. Pegau. 2007. Measurements of spectral optical properties and their relation to biogeochemical variables and processes in Crater Lake, Crater Lake National Park, OR. Hydrobiologia **574**: 149–159. doi:10.1007/s10750-006-2609-3

Bricaud, A., A. Morel, and L. Prieur. 1981. Absorption by dissolved organic matter of the sea (yellow substance) in the UV and visible domains. Limnol. Oceanogr. **26**: 43–53. doi:10.4319/lo.1981.26.1.0043

Bricaud, A., and D. Stramski. 1990. Spectral absorption coefficients of living phytoplankton and nonalgal biogenous matter: A comparison between the Peru upwelling area and the Sargasso Sea. Limnol. Oceanogr. **35**: 562–582. doi:10.4319/lo.1990.35.3.0562

Bricaud, A., M. Babin, A. Morel, and H. Claustre. 1995. Variability of chlorophyll specific absorption coefficient of natural phytoplankton: Analysis and parameterization. J. Geophys. Res. **100**: 13321–13332. doi:10.1029/95JC00463

Bricaud, A., H. Claustre, J. Ras, and K. Oubelkheir. 2004. Natural variability of phytoplanktonic absorption in oceanic waters: Influence of the size structure of algal populations. J. Geophys. Res. **109**: C11010. doi:10.1029/2004JC002419

Campbell, L., and D. Vaulot. 1993. Photosynthetic picoplankton community structure in the subtropical North Pacific ocean near Hawaii (Station ALOHA). Deep-Sea Res. I **40**: 2043–2060. doi:10.1016/0967-0637(93)90044-4

Cetinić, I., M. J. Perry, N. T. Briggs, E. Kallin, E. A. D'Asaro, and C. M. Lee. 2012. Particulate organic carbon and inherent optical properties during 2008 North Atlantic Bloom Experiment. J. Geophys. Res. **117**: C06028. doi:10.1029/2011JC007771

Church, M. J., M. W. Lomas, and F. Muller-Karger. 2013. Sea change: Charting the course for biogeochemical ocean time-series research in a new millennium. Deep-Sea Res. Part II **93**: 2–15. doi:10.1016/j.dsr2.2013.01.035

Cirulis, J. T., A. Scott, and G. M. Ross. 2013. Management of oxidative stress by microalgae. Can. J. Physiol. Pharmacol. **91**: 15–21. doi:10.1139/cjpp-2012-2049

Corno, G., D. M. Karl, M. J. Church, R. M. Letelier, R. Lukas, R. R. Bidigare, and M. R. Abbott. 2007. Impact of climate forcing on ecosystem processes in the North Pacific

Subtropical Gyre. J. Geophys. Res. **112**: C04021. doi:10.1029/2006JC003730

Cullen, J. J., and M. R. Lewis. 1988. The kinetics of algal photoadaptation in the context of vertical mixing. J. Plankton Res. **10**: 1039–1063. doi:10.1093/plankt/10.5.1039

Davis, R. F., C. C. Moore, J. R. V. Zaneveld, and J. M. Napp. 1997. Reducing the effects of fouling on chlorophyll estimates derived from long-term deployments of optical instruments. J. Geophys. Res. **102**: 5851–5855. doi:10.1029/96JC02430

DeLong, E. F., and O. Béjà. 2010. The light-driven proton pump proteorhodopsin enhances bacterial survival during tough times. PLoS Biol. **8**: e1000359. doi:10.1371/journal.pbio.1000359

Deming-Adams, B. 1990. Carotenoids and photoprotection in plants: A role for the xanthophyll zeaxanthin. Biochim. Biophys. Acta **1020**: 1−24. doi:10.1016/0005-2728(90)90088-L

Demers, S., S. Roy, R. Gagnon, and C. Vignault. 1991. Rapid light-induced changes in cell fluorescence and in xanthophyll-cycle pigments of *Alexandrium excavatum* (Dinophyceae) and *Thalassiosira pseudonana* (Bacillariophyceae): A photoprotection mechanism. Mar. Ecol. Prog. Ser. **76**: 185–193. doi:10.3354/meps076185

Dubinsky, Z. 1992. The functional and optical absorption cross-sections of phytoplankton photosynthesis, p. 31–45. *In* P. G. Falkowski, and A. D. Woodhead [eds.], Primary productivity and byogeochemical cycles in the sea. Plenum Press.

Emerson, R. 1958. The quantum yield of photosynthesis. Annu. Rev. Plant Physiol. **9**: 1–24. doi:10.1146/annurev.pp.09.060158.000245

Falkowski, P. G., and J. LaRoche. 1991. Acclimation to spectral irradiance by algae. J. Phycol. **27**: 8–14. doi:10.1111/j.0022-3646.1991.00008.x

Ferris, J. M., and R. Christian. 1991. Aquatic primary production in relation to microalgal responses to changing light: A review. Aquat. Sci. **53**: 187–217. doi:10.1007/BF00877059

Geider, R. J., H. L. MacIntyre, and T. M. Kana. 1997. Dynamic model of phytoplankton growth and acclimation: Responses of the balanced growth rate and chlorophyll *a*: Carbon ratio to light, nutrient-limitation and temperature. Mar. Ecol. Prog. Ser. **148**: 187–200. doi:10.3354/meps148187

Helbling, E. W., V. Villafañe, M. Ferrairo, and O. Holm-Hansen. 1992. Impact of natural ultraviolet radiation on rates of photosynthesis and on specific marine phytoplankton species. Mar. Ecol. Prog. Ser. **80**: 89–100. doi:10.3354/meps080089

Huisman, J., N. N. Pham Thi, D. M. Karl, and B. Sommeijer. 2006. Reduced mixing generates oscillations and chaos in the oceanic deep chlorophyll maximum. Nature **439**: 322–325. doi:10.1038/nature04245

Karl, D. M., and R. Lukas. 1996. The Hawaii Ocean Time-series (HOT) program: Background, rationale and field implementation. Deep-Sea Res. Part II **43**: 129–156. doi:10.1016/0967-0645(96)00005-7

Karl, D. M., D. V. Hebel, K. Björkman, and R. M. Letelier. 1998. The role of dissolved organic matter release in the productivity of the oligotrophic North Pacific Ocean. Limnol. Oceanogr. **43**: 1270–1286. doi:10.4319/lo.1998.43.6.1270

Karl, D. M., R. Bidigare, and R. M. Letelier. 2001. Long-term changes in plankton community structure and productivity in the North Pacific Subtropical Gyre: The domain shift hypothesis. Deep-Sea Res. Part II **48**: 1449−01470. doi:10.1016/S0967-0645(00)00149-1

Karl, D. M., R. Bidigare, and R. M. Letelier. 2002. Sustained seasonal and interannual variability of phytoplankton processes in the North Pacific Subtropical Gyre, p. 222–264. *In* P. J. LeB. Williams D. N. Thomas, and C. Reynolds [eds.], Phytoplankton productivity: Carbon assimilation in marine and freshwaters ecosystems. Blackwell Science Ltd.

Ketchum, B. H., J. H. Ryther, C. S. Yentsch, and N. Corwin. 1958. Productivity in relation to nutrients. Rapp. P.-V. Reun. Cons. Perm. Int. Explor. Mer. **144**: 132–140. doi:10.1371/journal.pbio.1000359

Kirk, T. O. 1994. Light and photosynthesis in aquatic ecosystems. 2nd ed. Cambridge Univ. Press.

Kishino, M., N. Okami, M. Takahashi, and S. Ichimura. 1986. Light utilization efficiency and quantum yield of phytoplankton in a thermally stratified sea. Limnol. Oceanogr. **31**: 557–566. doi:10.1371/journal.pbio.1000359

Latasa, M. 1995. Pigment composition of *Heterocapsa sp*. And *Thalassiosira weissflogii* growing in batch cultures under different irradiances. Sci. Mar. **59**: 25–37.

Latasa, M., and E. Berdalet. 1994. Effect on nitrogen or phosphorus starvation on pigment composition of cultured *Heterocapsa sp*. J. Plankton Res. **16**: 83–94. doi:10.1093/plankt/16.1.83

Latasa, M., M. R. Landry, L. Schlueter, and R. R. Bidigare. 1997. Pigment-specific growth and grazing rates of phytoplankton in the central equatorial Pacific. Limnol. Oceanogr. **42**: 289–298. doi:10.4319/lo.1997.42.2.0289

Le, C., Y. Li, Y. Zha, and D. Sun. 2008. Specific absorption coefficient and the phytoplankton package effect in Lake Taihu, China. Hydrobiologia **619**: 27–37. doi:10.1007/s10750-008-9579-6

Letelier, R. M., R. R. Bidigare, D. V. Hebel, M. Ondrusek, C. D. Winn, and D. M. Karl. 1993. Temporal variability of phytoplankton community structure based in pigment analysis. Limnol. Oceanogr. **38**: 1420–1437. doi:10.4319/lo.1993.38.7.1420

Letelier, R. M., J. E. Dore, C. D. Winn, and D. M. Karl. 1996. Seasonal and interannual variations in photosynthetic carbon assimilation at Station ALOHA. Deep-Sea Res. Part II **43**: 467–490. doi:10.1016/0967-0645(96)00006-9

Letelier, R. M., and D. M. Karl. 1996. The role of *Trichodesmium spp*. in the productivity of the subtropical North

Pacific Ocean. Mar. Ecol. Prog. Ser. **133**: 263–273. doi:10.3354/meps133263

Letelier, R. M., D. M. Karl, M. R. Abbott, and R. R. Bidigare. 2004. Light driven seasonal patterns of chlorophyll and nitrate in the lower euphotic zone of the North Pacific Subtropical Gyre. Limnol. Oceanogr. **49**: 508–519. doi:10.4319/lo.2004.49.2.0508

Lin, H., F. I. Kuzminov, J. Park, S. Lee, P. G. Falkowski, and M. Y. Gorbunov. 2016. The fate of photons absorbed by phytoplankton in the global ocean. Science **351**: 264–267. doi:10.1126/science.aab2213

Mackey, K. R. M., A. Paytan, A. R. Grossman, and S. Bailey. 2008. A photosynthetic strategy for coping in a high-light, low nutrient environment. Limnol. Oceanogr. **53**: 900–913. doi:10.4319/lo.2008.53.3.0900

Madariaga, I., and I. Joint. 1992. A comparative study of phytoplankton physiological indicators. J. Exp. Mar. Biol. Ecol. **158**: 149–165. doi:10.1016/0022-0981(92)90223-W

Malmstrom, R. R., A. Coe, G. C. Kettler, A. C. Martiny, J. Frias-Lopez, E. R. Zinser, and S. W. Chisholm. 2010. Temporal dynamics of *Prochlorococcus* ecotypes in the Atlantic and Pacific oceans. IMSE J **4**: 1252–1264. doi:10.1038/ismej.2010.60

Margalef, R. 1978. Life-forms of phytoplankton as survival alternatives in an unstable environment. Oceanol. Acta **1**: 493–509.

Markager, S., and F. V. Warwick. 2001. Light absorption by phytoplankton: Development of a matching parameter for algal photosynthesis under different spectral regimes. J. Plankton Res. **23**: 1373–1384. doi:10.1093/plankt/23.12.1373

Marra, J., C. C. Trees, R. R. Bidigare, and R. T. Barber. 2000. Pigment absorption and quantum yields in the Arabian Sea. Deep-Sea Res. Part II **47**: 1279–1299. doi:10.1016/S0967-0645(99)00144-7

Mitchell, B. G. 1990. Algorithms for determining the absorption coefficient of aquatic particulates using the quantitative filter technique (QFT), p. 137–148. *In* M. A. Blizard [ed.], Ocean optics VII. SPIE.

Montecino, V., and G. Pizarro. 1995. Phytoplankton acclimation and spectral penetration of UV irradiance off the central Chilean coast. Mar. Ecol. Prog. Ser. **121**: 261–269. doi:10.3354/meps121261

Moore, C. M., and others. 2013. Processes and patterns of oceanic nutrient limitation. Nat. Geosci. **6**: 701–710. doi:10.1038/NGEO1765

Moore, L. R., R. Georicke, and S. W. Chisholm. 1995. Comparative physiology of *Synechococcus* and *Prochlorococcus*: Influence of light and temperature on growth, pigments, fluorescence and absorptive properties. Mar. Ecol. Prog. Ser. **116**: 259–275. doi:10.3354/meps116259

Morel, A. 1978. Available, usable, and stored radiant energy in relation to marine photosynthesis. Deep-Sea Res. I **25**: 673–688. doi:10.1016/0146-6291(78)90623-9

Morel, A., and A. Bricaud. 1981. Theoretical results concerning light absorption in a discrete medium and applications to specific absorption of phytoplankton. Deep-Sea Res. I **28**: 1375–1393. doi:10.1016/0198-0149(81)90039-X

Nelson, N. B., B. B. Prezelin, and R. R. Bidigare. 1993. Phytoplankton light absorption and packaging effect in California coastal waters. Mar. Ecol. Prog. Ser. **94**: 217–227. doi:10.3354/meps094217

Oxborough, K., C. M. Moore, D. J. Suggett, T. Lawson, H. G. Chan, and R. J. Geider. 2012. Direct estimation of functional PSII reaction center concentration and PSII electron flux on a volume basis: A new approach to the analysis of Fast Repetition Rate fluorometry (FRRf) data. Limnol. Oceanogr.: Methods **10**: 142–154. doi:10.4319/lom.2012.10.142

Přibyl, P., J. Pilný, V. Cepák, and P. Kaštánek. 2016. The role of light and nitrogen in growth and carotenoid accumulation in *Scenedesmus* sp. Algal Res. **16**: 69–75. doi:10.1016/j.algal.2016.02.028

Quay, P. D., C. Peacock, K. Björkman, and D. M. Karl. 2010. Measuring primary production rates in the ocean: Enigmatic results between incubation and non-incubation methods at Station ALOHA. Global Biogeochem. Cycles **24**: GB3014. doi:10.1029/2009GB003665

Raven, J. A., and R. J. Geider. 2003. Adaptation, acclimation and regulation in algal photosynthesis, p. 385–412. *In* A. W. Larkum, S. E. Douglas, and J. A. Raven [eds.], Photosynthesis in algae. Kluwer Academic Publishers.

Reigman, R., and A. Rowe. 1994. Nutritional status and pigment composition of phytoplankton during spring and summer *Phaeocystis* blooms in Dutch coastal waters (Marsdiep area). Neth. J. Sea Res. **32**: 13–21. doi:10.1016/0077-7579(94)90024-8

Roesler, C. S. 1998. Theoretical and experimental approaches to improve the accuracy of particulate absorption coefficients from the Quantitative Filter Technique. Limnol. Oceanogr. **43**: 1649–1660. doi:10.4319/lo.1998.43.7.1649

Sakshaug, E. A., and others. 1997. Parameters of photosynthesis: Definitions, theory and interpretation of results. J. Plankton Res. 1637–1670. doi:10.1093/plankt/19.11.1637

Schlüter, L., B. Reimann, and M. Søndergaard. 1997. Nutrient limitation in relation to phytoplankton carotenoid/chlorophyll *a* ratios in freshwater mesocosms. J. Plankton Res. **19**: 891–906. doi:10.1093/plankt/19.7.891

Smith, R. C., J. Marra, M. J. Perry, K. S. Baker, E. Swift, E. Buskey, and D. A. Kiefer. 1989. Estimation of a photon budget for the upper ocean in the Sargasso Sea. Limnol. Oceanogr. **34**: 1673–1693. doi:10.4319/lo.1989.34.8.1673

Sosik, H. M., and B. G. Mitchell. 1995. Light absorption by phytoplankton, photosynthetic pigments and detritus in the California Current System. Deep-Sea Res. I **42**: 1717–1748. doi:10.1016/0967-0637(95)00081-G

Staehr, P. A., P. Henriksen, and S. Markager. 2002. Photoacclimation of four marine phytoplankton species to

irradiance and nutrient availability. Mar. Ecol. Prog. Ser. **238**: 47–59. doi:10.3354/meps238047

Suttle, C. A. 2000. The ecological, evolutionary and geochemical consequences of viral infection of cyanobacteria and eukaryotic algae, p. 247–296. *In* C. J. Hurst [ed.], Viral ecology. Academic Press.

Watson, R. A., and P. L. Osborne. 1979. Algal pigment ratio as an indicator of the nitrogen supply to phytoplankton in three Norfolk broads. Freshw. Biol. **9**: 585–594. doi: 10.1111/j.1365-2427.1979.tb01541.x

Winn, C. D., L. Campbell, J. R. Christian, R. M. Letelier, D. V. Hebel, J. E. Dore, L. Fujieki, and D. M. Karl. 1995. Seasonal variability in the phytoplankton community of the North Pacific Subtropical Gyre. Global Biogeochem. Cycles **9**: 605–620. doi:10.1029/95GB02149

Woźniak, B., J. Debra, D. Ficek, R. Majchrowski, S. Kaczmarek, M. Ostrowska, and O. I. Klobentz-MisHke. 1999. Modelling the influence of acclimation on the absorption properties of marine phytoplankton. Oceanologia **41**: 187–210.

Woźniak, B., J. Debra, D. Ficek, R. Majchrowski, S. Kaczmarek, M. Ostrowska, and O. I. Klobentz-MisHke. 2000. Model of the 'in vivo'; spectral absorption of algal pigments. Part 1. Mathematical apparatus. Oceanologia **42**: 177–190.

Woźniak, B., J. Dera, D. Ficek, R. Majchrowski, M. Ostrowska, and S. Kaczmarek. 2003. Modelling light and photosynthesis in the marine environment. Oceanologia **45**: 171–245.

Yentsch, C. S., and R. F. Vaccaro. 1958. Phytoplankton nitrogen in the oceans. Limnol. Oceanogr. **3**: 443–448. doi: 10.4319/lo.1958.3.4.0443

Acknowledgments

We are indebted to the captains and crews of the various research vessels involved in supporting the Hawaii Ocean Time-series (HOT) program. In addition, we acknowledge the dedicated efforts of the HOT program staff for sample collections and processing; Jasmine Nahorniak and Amanda Whitmire were instrumental in the processing of the optical data while Marnie Jo Zirbel and Julie Arrington ran the filter pad absorption samples. Two anonymous reviewers provided valuable comments on the manuscript. Support was provided by the National Science Foundation (HOT, OCE-1260164 and C-MORE, EF-0424599), the Gordon and Betty Moore Foundation's Marine Microbiology Initiative (DMK, grant #3794), the Simons Foundation (Simons Collaboration on Ocean Processes and Ecology Award 329108; DMK, AEW, MJC) and the Balzan Foundation (DMK).

Conflict of Interest

None declared.

Submitted 05 July 2016
Revised 01 November 2016
Accepted 15 December 2016

Associate editor: David Antoine